Title

Mouse cytomegalovirus-experienced ILC1s acquire a memory response dependent on the viral glycoprotein m12.

Journal

Nature immunology, 20(8)

ISSN

1529-2908

Authors

Weizman, Orr-El
Song, Eric
Adams, Nicholas M
et al.

Publication Date

2019-08-01

DOI

10.1038/s41590-019-0430-1

Peer reviewed

HHS Public Access

Author manuscript

Nat Immunol. Author manuscript; available in PMC 2020 January 01.

Published in final edited form as:

Nat Immunol. 2019 August ; 20(8): 1004–1011. doi:10.1038/s41590-019-0430-1.

Mouse cytomegalovirus-experienced ILC1s acquire a memory response dependent on the viral glycoprotein m12

Orr-El Weizman[1,2], **Eric Song**[2], **Nicholas M. Adams**[1,3], **Andrew D. Hildreth**[4,5], **Luke Riggan**[4,5], **Chirag Krishna**[6], **Oscar A. Aguilar**[7,#], **Christina S. Leslie**[6], **James R. Carlyle**[7], **Joseph C. Sun**[1,3,8], **Timothy E. O'Sullivan**[4,5,*]

[1]Immunology Program, Memorial Sloan Kettering Cancer Center, New York, NY, 10065, USA

[2]Department of Immunobiology, Yale University, New Haven, CT, 06511, USA

[3]Louis V. Gerstner, Jr. Graduate School of Biomedical Sciences, Memorial Sloan Kettering Cancer Center, New York, NY 10065, USA

[4]Department of Microbiology, Immunology, and Molecular Genetics, David Geffen School of Medicine at UCLA, Los Angeles, CA 900953

[5]Molecular Biology Institute, University of California, Los Angeles, Los Angeles, CA 90095, USA

[6]Computational and Systems Biology Program, Memorial Sloan Kettering Cancer Center, New York, NY, 10065, USA

[7]Department of Immunology, University of Toronto, Toronto, ON M5S 1A8, Canada

[8]Department of Immunology and Microbial Pathogenesis, Weill Cornell Medical College, New York, NY 10065, USA

Abstract

Innate lymphoid cells (ILCs) are tissue-resident sentinels that are essential for early host protection from pathogens at initial sites of infection. However, whether pathogen-derived antigens directly modulate the responses of tissue-resident ILCs has remained unclear. Here, we found that liver-resident type 1 innate lymphoid cells (ILC1s) expanded locally and persisted after the resolution of infection with mouse cytomegalovirus (MCMV). ILC1s acquired stable transcriptional, epigenetic and phenotypic changes a month after the resolution of MCMV infection, and showed an enhanced protective effector response to secondary challenge with

[*]*Corresponding Author* Timothy E. O'Sullivan, PhD, David Geffen School of Medicine at UCLA, 615 Charles E. Young Drive South, BSRB 245F, Los Angeles, CA 90095, Phone: 310-825-4454, tosullivan@mednet.ucla.edu.

[#]Present Address: Department of Microbiology and Immunology, University of California, San Francisco, San Francisco, CA 94143, USA

Author Contributions

O.E.W, and T.E.O. designed the study; O.E.W, N.M.A., A.D.H., L.R., and T.E.O performed the experiments; E.S., C.K., and C.S.L. performed RNA-seq and ATAC-seq bioinformatics analysis; J.R.C. and O.A.A. provided reagents; O.E.W, J.C.S. and T.E.O. wrote the manuscript.

The authors declare no financial conflicts of interest.

Competing Interests Statement

The authors declare no competing interests.

MCMV consistent with a memory lymphocyte response. Memory ILC1 responses were dependent on the MCMV-encoded glycoprotein m12, and were independent of bystander activation by proinflammatory cytokines after heterologous infection. Thus, liver ILC1s acquire adaptive features in an MCMV-specific manner.

The ability of an organism to "remember" previous pathogen encounters by mounting a specific and robust secondary response upon re-exposure to pathogen-associated antigens is termed "immunological memory". During infection, this memory response is largely coordinated by the selective clonal proliferation and long-term persistence of adaptive lymphocytes that express somatically recombined antigen receptors (e.g. T cells) to form antigen-specific memory cells that are able to epigenetically maintain activation-induced transcriptional changes following the clearance of pathogen[1, 2]. Coordination of stable epigenetic, transcriptional and metabolic changes in adaptive memory cells results in cell-intrinsic increases in cytotoxic potential and proinflammatory cytokine production upon secondary pathogen exposure to enhance host protection[1, 3, 4]. A robust host-protective memory response requires the coordinated contributions of circulating and tissue-resident memory T cells (T_{RM}). Following primary viral infection, circulating virus-specific effector T cells can give rise to T_{RM} at the sites of initial pathogen encounter, which rapidly and robustly respond to secondary infection in an antigen-dependent manner[5]. While immunological memory is classically defined in an antigen-specific context, recent evidence suggests that circulating and tissue-resident cells of the innate immune system (e.g. natural killer (NK) cells, monocytes, group 2 innate lymphoid cells (ILCs)) can acquire enhanced effector function or stable activation-induced epigenetic changes following exposure to various inflammatory stimuli in an antigen-independent manner[6, 7, 8]. However, whether tissue-resident innate immune cells also have the potential to form antigen-dependent memory responses is unknown.

ILCs are tissue-resident innate immune cells that can be found in non-lymphoid tissues, and are enriched at epithelial barrier surfaces such as the intestine, lung and skin[9]. ILCs do not express rearranged antigen receptors, but instead express a wide variety of germline-encoded activating and inhibitory receptors[9, 10]. It is generally believed that ILCs lack the ability to respond to pathogen-derived antigens, but instead respond rapidly to proinflammatory signals within discrete tissue microenvironments in an antigen-independent manner[11]. Type 1 innate lymphocytes (ILC1s) are tissue-resident sentinels that function to protect the host from bacterial and viral pathogens at initial sites of infection[12, 13, 14]. ILC1s rapidly produce the cytokine IFN-γ following the local activation of dendritic cells and the production of the proinflammatory cytokine IL-12 to limit viral replication and promote host survival before the recruitment of circulating lymphocytes into infected tissues[12]. Studies in parabiotic mice have indicated that ILCs are not continuously replaced by bone marrow-derived precursors during steady-state or shortly after inflammation, and do not recirculate to other tissues[12, 15, 16, 17]. Instead, ILCs are thought to self-renew within tissues, suggesting that pathogen-experienced ILCs would persist following the resolution of inflammation. Given the essential role of ILC1 in host protection, whether ILC1 act as short-lived effector cells or persist and adapt following pathogen exposure remains unclear.

In this study, we demonstrate that liver ILC1s expanded and contracted following infection with mouse cytomegalovirus (MCMV) to form a stable pool of memory cells. A subset of memory ILC1s expressing the cytokine receptor IL-18Rα (hereafter IL-18R) displayed enhanced effector function following stimulation of NK1.1 or NKp46 *ex vivo* and reinfection with MCMV *in vivo*. RNA-seq and ATAC-seq analysis revealed that IL-18R$^+$ ILC1s maintained distinct and stable transcriptional and epigenetic signatures compared to naïve ILC1s. Furthermore, memory ILC1 responses were dependent on the MCMV-encoded glycoprotein m12, but not observed following heterologous infection. Thus, our study reveals that liver ILC1s can form memory responses in an antigen-dependent manner following MCMV infection.

Results

Liver ILC1s proliferate and persist following MCMV infection

Circulating natural killer (NK) cells can robustly proliferate, contract and persist as long-lived memory cells following infection with MCMV, exhibiting similar responses that have been previously observed in lymphocytes of the adaptive immune system[18]. To investigate the response of ILC1s following primary viral infection, C57BL/6 wild-type mice were infected with MCMV intraperitoneally (i.p). and the absolute numbers of CD45.2$^+$Lin$^-$NK1.1$^+$CD49b$^-$Eomes$^-$CD200r1$^+$ ILC1s (hereafter ILC1s) were analyzed in the liver at day 2, 7, 14, and 28 post-infection. Compared to uninfected mice, the number of ILC1s in the liver decreased on day 2 post-infection, concomitant with the increased incorporation of a fluorescently labeled caspase inhibitor (FLICA) (Fig 1a,b), suggesting that a proportion of ILC1s underwent apoptosis at this timepoint. In contrast, the absolute number of ILC1s in the liver increased on day 7 post-infection compared to uninfected mice (Fig. 1a). ILC1s had increased expression of the proliferation marker Ki67 on days 2, 4 and 7 post-infection compared to uninfected mice (Fig. 1c), and liver CD45.2$^+$Lin$^-$NK1.1$^+$CD49b$^-$CD200r1$^+$ILC1s (hereafter sorted ILC1s) adoptively transferred into CD45.1 wild-type recipient mice diluted cell proliferation tracing dye (CTV) and underwent a ~5 fold expansion on day 7 post-infection compared to sorted CD45.2$^+$ ILC1s transferred into uninfected CD45.1 mice (Fig. 1d,e). These results suggested that ILC1s in the liver proliferated between day 2 and day 7 post-infection. At day 9 post-infection, ILC1s in the liver had similar expression of Ki67, but increased incorporation of FLICA compared to ILC1s in the liver of uninfected mice (Fig. 1b,c). Coupled with the decrease in absolute numbers of ILC1s in the liver on day 14 and day 30 post-infection compared to day 7 (Fig. 1a), these observations suggested that ILC1s underwent a contraction phase following the resolution of infection from day 7 to day 30 post-infection. To test whether ILC1s persisted following the resolution of MCMV infection, we sorted CD45.2$^+$ ILC1s from the liver of wild-type mice and adoptively-transferred them into CD45.1 wild-type mice, which were subsequently infected i.p with MCMV one day after transfer or left uninfected. Transferred CD45.2$^+$ ILC1s were recovered from both MCMV-infected and uninfected hosts 30 days after transfer (Fig. 1f,g), suggesting that ILC1s were maintained long-term during homeostasis and after viral infection. These results indicate that ILC1s in the liver went through distinct phases of proliferation, contraction and persistence following infection with MCMV.

ILC1s require proinflammatory cytokine signaling for local proliferation

The proliferation of effector NK cells in response to MCMV is mediated by recognition of the MCMV-encoded glycoprotein m157 by the germline encoded activating receptor Ly49H (*Klra8*), proinflammatory cytokines such as IL-12 and IL-18, and the transcription factor *Zbtb32*[6, 18, 19, 20]. We investigated whether these signals were required for the proliferation of ILC1s during MCMV infection by generating mixed bone marrow chimeric mice obtained by co transferring wild-type CD45.1$^+$ bone marrow with either *Klra8*$^{-/-}$, *Il12rb2*$^{-/-}$*Il18r1*$^{-/-}$ or *Zbtb32*$^{-/-}$ (CD45.2$^+$) bone marrow at a 1:1 ratio into CD45.1 xCD45.2 wild-type recipients (hereafter *Klra8*$^{-/-}$ mBMC, *Il12rb2*$^{-/-}$*Il18r1*$^{-/-}$ mBMC, and *Zbtb32*$^{-/-}$ mBMC respectively). After MCMV infection of mBMC mice, the frequency of *Il12rb2*$^{-/-}$*Il18r1*$^{-/-}$ ILC1s and *Zbtb32*$^{-/-}$ ILC1s was (70–80%) lower than wild-type ILC1s in the liver of *Il12rb2*$^{-/-}$*Il18r1*$^{-/-}$ and *Zbtb32*$^{-/-}$ mBMC mice respectively at day 7 post-infection (Fig. 2a), indicating that similar to NK cells, the MCMV-induced accumulation of ILC1s in the liver was dependent on IL-12-IL-18 and Zbtb32 signaling in a cell-intrinsic manner. In contrast, the frequency of *Klra8*$^{-/-}$ ILC1s was equivalent to wild-type ILC1 in the liver of *Klra8*$^{-/-}$ mBMC at day 7 post-infection (Fig. 2a), indicating that Ly49H was dispensable for ILC1 proliferation after MCMV infection. ILC1s are thought to be phenotypically and functionally stable during viral infections[12, 21]. To test whether the ILC1s in the liver at day 30 after MCMV infection were derived from a pool of immature NK cells that downregulated the expression of Ly49H after infection, we sorted ILC1s from the liver of CD45.2 wild-type mice (Supplementary Fig. 1a) and adoptively-transferred them into CD45.1 *Klar8*$^{-/-}$ mice that were infected with MCMV i.p one day after adoptive transfer. One week post-infection, recovered CD45.2$^+$ ILC1s in the liver did not express the effector NK cell markers KLRG1 or CD11b, the NK cell lineage-defining markers Eomes or CD49b or the activating receptors Ly49H or Ly49D compared to Lin$^-$NK1.1$^+$CD49b$^+$Eomes$^+$CD200r1$^-$ NK cells (hereafter NK cells) or ILC1s in the liver of uninfected wild-type mice (Fig. 2b **and** Supplementary Fig. 1b). To directly test whether ILC1s in the liver remained tissue-resident and were not replenished from the circulation, we generated parabiotic mice by surgically connecting the vasculature of CD45.1 and CD45.2 wild-type mice for 30 days until complete donor chimerism of NK cells was established in peripheral blood (~50:50 ratio of CD45.1$^+$ to CD45.2$^+$ cells) (Fig. 2c). Following complete chimerism after ~4 weeks, both parabionts were infected with MCMV i.p. and the frequency of donor derived ILC1s and NK cells at day 7 and day 28 post-infection was analyzed. ILC1s in the liver were ~95% host-derived at day 7 and day 28 post-infection, whereas NK cells were derived equally from both parabionts in the spleen, liver and peripheral blood (Fig. 2c). These data suggest that MCMV-induced proinflammatory signals were required to drive the local proliferation of a phenotypically stable lineage of liver ILC1s.

MCMV infection impacts the phenotypic and functional properties of ILC1s

Memory CD8$^+$ T cells (T_M cells), CD4$^+$ T_M cells and regulatory T cells (T_{reg} cells) have increased expression of *Il7r, Il2ra* and *Il18r1* transcripts compared to naïve T cells (Supplementary Fig. 2)[4, 22, 23]. T_M cells require IL-15 and IL-7 for their survival and persistence during homeostasis[24, 25], and IL-18 to mediate optimal recall responses during viral and bacterial challenges[26, 27]. We investigated whether MCMV-experienced liver

ILC1s had phenotypic properties similar to that of adaptive memory lymphocytes. ILC1s in the liver had increased cell surface expression of IL-7Rα (hereafter IL-7R), IL-2Rα (hereafter IL-2R) and IL-18R 30 days after MCMV infection compared to uninfected mice (Fig. 3a-c). At this time point after MCMV infection, ILC1s in the liver exhibited a bimodal expression of IL-18R (Fig. 3c). To determine whether naïve ILC1s induce the expression of IL-18R after MCMV infection, we transferred IL-18R$^-$ ILC1s sorted from the liver of CD45.2 wild-type mice i.v. into CD45.1 wild-type mice, and infected recipients with MCMV i.p. one day after transfer. On day 7 post-infection, 40% of CD45.2$^+$ IL-18R$^-$ ILC1s in the liver of recipient mice were IL-18R$^+$ (Fig. 3d), indicating that a subset of naïve IL-18R$^-$ ILC1s can induce IL-18R expression following MCMV infection. To assess the stability of IL-18R expression on ILC1s, IL-18R$^+$ ILC1s were sorted from the liver of CD45.2 wild-type mice on day 30 post-MCMV infection and adoptively transferred i.v. into naïve CD45.1 wild-type hosts. On day 3 after transfer, CD45.2$^+$ IL-18R$^+$ ILC1s recovered from the liver of CD45.1 recipient mice were IL-18R$^+$ (Fig. 3e), suggesting that IL-18R$^+$ ILC1 were phenotypically stable during homeostasis. Collectively, these data indicate that MCMV-experienced ILC1s acquired phenotypic markers similar to those induced on antigen-specific T_M cells after pathogen challenge.

Another hallmark of adaptive immunity is enhanced effector function upon secondary exposure to activating stimuli. IL-18R$^+$ ILC1s from the liver of wild-type mice 30 days after i.p. MCMV infection produced more IFN-γ after *ex-vivo* stimulation with plate-bound antibodies against the activating receptors NK1.1 or NKp46 compared to NK cells or IL-18R$^-$ ILC1s isolated from the liver of uninfected or MCMV-infected wild-type mice 30 days post-infection (Fig. 4a & Supplementary Figure 3). To investigate whether IL-18R$^+$ ILC1s displayed enhanced secondary effector responses following pathogen rechallenge *in vivo*, *Rag2*$^{-/-}$ mice were immunized i.p. with MCMV or control PBS, and then reinfected with MCMV hydrodynamically (h.d.) 28 days after primary infection. *Ex vivo* IFN-γ production was subsequently measured by flow cytometry following incubation with the Golgi complex inhibitor brefeldin A (BFA) *ex vivo* for 4 h. IFN-γ production was similar between IL-18R$^-$ ILC1s and IL-18R$^+$ ILC1s isolated from the liver of *Rag2*$^{-/-}$ mice 24 h after primary MCMV infection (Fig. 4b,c). However, IL-18R$^+$ ILC1s, but not IL-18R$^-$ ILC1s had enhanced production of IFN-γ 24 h after secondary infection (Fig. 4b,c), suggesting IL-18R$^+$ ILC1s had enhanced effector responses to pathogen rechallenge *in vivo*. Together, these results demonstrate that MCMV infection induced stable phenotypic and functional attributes in a subset of liver-resident ILC1.

IL-18R$^+$ ILC1s have a distinct transcriptional and epigenetic landscape

Memory lymphocytes have distinct transcriptional and epigenetic changes compared to their naïve counterparts that underpin their enhanced responsiveness to secondary stimulation[22, 23, 28, 29, 30, 31]. To determine if IL-18R$^+$ ILC1s showed unique transcriptional and epigenetic signatures after MCMV infection, we sorted ILC1s from the liver of naïve mice (naïve ILC1s hereafter) and IL-18R$^+$ ILC1s from the liver of MCMV-infected mice on day 35 post-infection (day 35 IL-18R$^+$ ILC1s hereafter) and performed RNA sequencing (RNA-seq) and ATAC sequencing (ATAC-seq). RNA-seq analysis identified 308 genes more highly expressed in naïve ILC1s compared to day 35 IL-18R$^+$ ILC1s (FDR adjusted $p<0.05$,

absLog2FC >1) and 805 genes more highly expressed in day 35 IL-18R$^+$ ILC1s compared to naïve ILC1s (FDR adjusted p<0.05, absLog2FC >1) (Fig. 5a and Supplementary Table 1). Day 35 IL-18R$^+$ ILC1s had increased expression of transcripts for *Ifng*, the transcription factors *Rora* and *Tcf7* and cytokine receptors *(Ifngr, Il2ra, Il18r1* and *Il7r)* compared to naïve ILC1s (Fig. 5b). Transcripts with increased expression in day 35 IL-18R$^+$ ILC1s compared to naive ILC1s were compared to genes associated with various T_M cell subsets induced by viral challenge from previously published genome-wide analyses using gene set enrichment analysis (GSEA)[32]. GSEA results showed a higher association of genes expressed in day 35 IL-18R$^+$ ILC1s with genes preferentially expressed in effector and resident CD8$^+$ T_M cells compared to naïve CD8$^+$ T cells (Supplementary Fig. 4a). Next, we generated a core 'lymphocyte memory' signature including genes that were significantly increased in day 35 IL-18R$^+$ ILC1s compared to naïve ILC1s and shared with effector, central and resident CD8$^+$ T_M cells compared to naïve CD8$^+$ T cells and ILC1s (FDR adjusted p<0.05, absLog2FC >1) (Fig. 5c). This signature of genes included transcription factors *(Runx3, Rora*), the metabolic enzyme *Arg1,* the effector molecule *Tnf,* the autophagy protein *Bag3*, the Wnt pathway regulator *Dkk1*, zinc finger family proteins (*Zfp523*, *Zfp579*, *Zfp692*) and cytokine receptors (*Il18r1, Il7r, Il2ra*). The core lymphocyte memory signature was consistent with the phenotypic analysis of cytokine receptor protein expression on MCMV-primed liver ILC1s (Fig. 3a-c).

ATAC-seq identified an atlas of 23016 accessible regions, with 373 significantly differentially accessible (DA) peaks between naïve ILC1s and day 35 IL-18R$^+$ ILC1s (FDR p<0.2) (Supplementary Fig. S4b,c). Of the 373 DA peaks, 282 peaks were more highly accessible in naïve ILC1s compared to day 35 IL-18R$^+$ ILC1s, and 91 peaks were more accessible in day 35 IL-18R$^+$ ILC1s compared to naïve ILC1s (FDR p<0.2) (Fig. 5d & Supplementary Fig. 4c). Day 35 IL-18R$^+$ ILC1s had increased accessibility for transcription factors (*Rora, Klf2, Etv6),* cell-adhesion molecules (*Itgb2, Itgb3),* and cytokine receptors *(Il7r* and *Ifnar*) compared to naïve ILC1s (Fig. 5e,f). For certain genes (*Il7r* and *Rora)* there was increased accessibility in the transcriptional start sites of these genes with a concomitant increase in transcripts in day 35 IL-18R$^+$ ILC1s compared to naïve ILC1s (Fig. 5b,f **and** Supplementary Fig. 4d), suggesting that subsets of DA genes were maintained in an enhanced transcriptional state in day 35 IL-18R$^+$ ILC1s compared to naive ILC1s.

m12 is required for the induction of IL-18R$^+$ ILC1s in the liver

Because lymphocyte memory responses can be antigen-dependent or antigen-indepedent[6, 7], we investigated the recall specificity of IL-18R$^+$ ILC1s in a heterologous infection model. Wild-type mice were primed intranasally (i.n.) with MCMV or PBS and subsequently challenged i.n. with influenza (PR-8 strain) 28 days after primary MCMV or mock infection. *Ex vivo* intracellular IFN-γ production of lung ILC1s following BFA incubation in MCMV-primed mice infected with influenza were similar to those measured in PBS-primed mice infected with influenza 48 h post-infection (Fig. 6a), suggesting that the increased secondary ILC1 IFN-γ responses previously observed in MCMV-primed mice were specific to MCMV reinfection. Next, we tested whether IL-12 and IL-18 stimulation alone were sufficient to drive heightened IFN-γ responses in MCMV-experienced ILC1s. *Ex vivo* stimulation for four hours with IL-12 and IL-18 did not induce enhanced IFN-γ production in NK cells,

IL-18R^{-} ILC1s or IL-18R^{+} ILC1s isolated from the liver of MCMV-infected wild-type mice on day 35 post-infection compared to naïve ILC1s from the liver of uninfected wild-type mice (Fig. 6b). These results suggest that cytokine stimulation was not sufficient to drive enhanced IFN-γ production in IL-18R^{+} ILC1s. Furthermore, wild-type mice primed intranasally (i.n.) with influenza or left uninfected and subsequently challenged i.n. with either MCMV or Sendai virus i.n. 28 days after primary influenza or mock infection had similar *ex vivo* IFN-γ production measured by flow cytometry in the lung 48 h after secondary i.n. infection (Supplementary Fig. S5a,b). Taken together, these results suggested that MCMV-primed IL-18R^{+} ILC1s responses may require MCMV-derived signals for enhanced secondary effector responses *in vivo*.

Because liver ILC1s expressed a limited repertoire of activating and inhibitory receptors (*Klrb1b*, *Klrb1c*, *Klrb1a*) that could be specific for known MCMV-encoded antigens (Supplementary Fig. 6a), and ex-vivo stimulation with antibodies against NK1.1 (*Klrb1c*) enhanced IFN-γ responses in IL-18R^{+} ILC1s (Fig. 4a), we tested whether the NKR-P1 (Klrb) family ligand m12, an MCMV encoded immunoevasin[33], drove the induction of IL-18R^{+} ILC1s through the stimulation of *Klrb1c* or *Klrb1a* receptors. We infected wild-type mice i.p. with a MCMV Smith strain (hereafter Smith), a MCMV MW97 mutant strain deficient in m12 (hereafter Δm12) or an MCMV MW97 mutant expressing MCMV Smith m12 ortholog (hereafter m12^{smith}), and measured the frequency of IL-18R^{+} ILC1s in the liver at day 30 post-infection. Infection with m12^{smith} induced a similar frequency of IL-18R^{+} ILC1s (~50%) compared to infection with Smith (~50%) (Fig. 6c), while infection with Δm12 did not generate IL-18R^{+} ILC1s in the liver (Fig. 6c). Furthermore, only i.p. infection with Smith or m12^{smith} MCMV induced enhanced IFN-γ production after *ex vivo* stimulation with NK1.1 antibody in IL-18R^{+} ILC1s, but not in IL-18R^{-} ILC1s or NK cells, compared with to wild-type mice infected i.p. with Δm12 (Fig. 6d **and** Supplementary Fig. 6b,c). In addition, IL-18R^{+} ILC1s generated by primary infection with Smith or m12^{smith} in *Rag2*$^{-/-}$ mice and challenged 28 days later with Smith limited early viral replication in the liver 48 hours after secondary challenge to a greater extent than *Rag2*$^{-/-}$ mice primed with Δm12 (Fig. 6e). Thus, enhanced IFN-γ production and host protection by MCMV-experienced liver ILC1s was dependent on the MCMV-derived glycoprotein m12.

Discussion

Here we show that a subset of MCMV-experienced liver-resident ILC1s expressing the cytokine receptor IL-18R displayed enhanced effector function following stimulation of the activating receptor NK1.1 *ex vivo* and reinfection with MCMV *in vivo*. RNA-seq and ATAC-seq analysis revealed that IL-18R^{+} ILC1s maintained distinct and stable transcriptional and epigenetic signatures compared to naïve ILC1s. Furthermore, enhanced IL-18R^{+} ILC1 responses were dependent on the MCMV immunoevasin m12, but not observed following heterologous infection.

As a naturally occurring mouse pathogen, MCMV demonstrates evidence of co-evolution with its host through the expression of immunoevasive molecules that antagonize host activating receptors or stimulate inhibitory receptors[34]. During MCMV infection, T cells and NK cells each recognize unique MCMV-encoded antigens to generate an effective

lymphocyte memory pool[18, 35]. Unlike adaptive CD8$^+$ T cells, which use a somatically rearranged TCR to recognize viral peptides presented on MHC class I, NK cell expansion and memory formation is driven by the germline-encoded activating receptor Ly49H through recognition of the MCMV-encoded glycoprotein m157[18, 36]. Studies using hapten-induced contact hypersensitivity models have shown that hepatic ILCs with an ILC1-like phenotype can mediate recall responses to specific haptens in an antigen-specific manner[37, 38, 39], although the precise mechanisms responsible for the antigen-specificity of these cells remained unknown and the physiological significance of these memory responses remained poorly defined. Our studies extend these previous observations by demonstrating that liver-resident ILC1s recognized the MCMV-encoded glycoprotein m12 to drive the formation of an IL-18R$^+$ ILC1 subset consistent with a memory lymphocyte phenotype. These conclusions are based on the stable acquisition of distinct transcriptional, epigenetic, phenotypic and functional attributes observed in IL-18R$^+$ ILC1s compared to naïve ILC1 that result in cell-intrinsic increases in IFN-γ production upon secondary MCMV exposure to enhance host protection. These traits are consistent with current criteria to define memory lymphocytes[1, 3, 4].

The shared recognition of MCMV-encoded proteins by NK cells and ILC1s suggests a strong selective pressure for the host to evolve germline-encoded receptors to control subsequent MCMV encounters. Specifically, m12 can be recognized by both activating and inhibitory members of the NKR-P1 receptor family[33]. Our RNA-seq analysis indicated that liver ILC1s expressed *Klrb1a* (Nkrp1a), *Klrb1b* (Nkrp1b) and *Klrb1c* (Nkrp1c, NK1.1), all of which can signal in the presence of m12 *in vitro*. Stimulation of activating receptor NK1.1 resulted in enhanced IFN-γ production only in MCMV-experienced IL-18R$^+$ ILC1s, indicating that NK1.1 recognition of m12 and downstream signaling may be required for the generation of memory ILC1s. However, it remains possible that m12-induced Nkrp1b inhibitory receptor signaling in the presence of proinflammatory cytokines can achieve a specific priming signal to generate memory responses in liver ILC1s, or that both m12-induced Nkrp1a and NK1.1 activating signals can overcome Nkrp1b inhibitory signaling to prime liver ILC1 responses. Furthermore, we cannot exclude the possibility that IL-18R$^-$ ILC1s in MCMV-infected mice may have not been exposed to m12, offering a potential explanation for why these cells did not show enhanced IFN-γ production during reinfection. Although future work will be necessary to determine the specific receptors that mediate memory ILC1 responses, our study defines an essential role for m12 in this process. Thus, these findings leave open the possibility that other tissue-resident ILCs may express germline-encoded receptors with specificity to co-evolved pathogens to modify their effector responses during infection, although future work will be necessary to support this hypothesis.

Immunological memory is classically defined in an antigen-specific context; however, cells of the innate immune system can acquire stable epigenetic modifications and/or enhanced secondary effector function following exposure to various inflammatory stimuli in an antigen-independent manner[6, 7]. This process, referred by some as “cytokine-induced memory” and “trained immunity”, can be achieved in NK cells and monocytes through stimulation with the proinflammatory cytokines IL-12+IL-18 and *C. albicans*-derived β-glucan, respectively[40, 41]. Similarly, papain- or IL-33-stimulated lung ILC2s can display

enhanced effector recall responses upon challenge with unrelated allergens to enhance allergic pathology[8]. While these studies provide evidence that memory-like responses can be observed in various innate immune cell types, the importance of these responses towards host protection during pathogen challenge are still not well understood. Our results demonstrated that liver-resident memory ILC1s are not generated during heterologous infections that induce similar production of proinflammatory cytokines, and did not display enhanced IFN-γ production after *ex vivo* stimulation with IL-12 and IL-18. These findings are similar to results found with MCMV-specific Ly49H$^+$ NK cells[42], and suggest that m12-dependent memory ILC1s are distinct from antigen-independent innate immune memory responses and may be more analogous to adaptive T cell and NK cell memory responses.

Methods

Mice

Mice were bred at UCLA and Memorial Sloan Kettering Cancer Center in accordance with the guidelines of the institutional Animal Care and Use Committee (IACUC). The following mouse strains were used this study: C57BL/6 (CD45.2) (Jackson Labs, #000664), B6.SJL (CD45.1) (Jackson Labs, #002114), *Rag2*$^{-/-}$ (Jackson Labs #008449), *Klra8*$^{-/-}$ (Ly49H-deficient), *Zbtb32*$^{-/-}$, and *Il12rb2*$^{-/-}$ *x Il18ra1*$^{-/-}$ (MSKCC, J.C. Sun). Experiments were conducted using 7–8 week old age- and gender-matched mice in accordance with approved institutional protocols.

Generation of mixed bone marrow chimeric mice was performed as previously described[18]. Parabiosis surgery was performed as previously described[12, 15, 16, 17]. Intravascular labeling of lymphocytes of experimental mice was performed by injecting (i.v.) 2.5 μg of fluorophore-conjugated CD45 (30-F11) and euthanized 3 minutes later.

Viruses and In vivo Infection Models

MCMV (Smith) was serially passaged through BALB/c hosts three times, and then salivary gland viral stocks were prepared with a dounce homogenizer for dissociating the salivary glands of infected mice 3 weeks after infection. MW97.01 MCMV (m12-deficient and m12^{Smith}) virus were constructed using BAC technology and are described previously[33]. Sendai virus (Cantell strain) and Influenza virus (PR8 Strain) were grown in 10 day embryonated chicken eggs (SPAFAS; Charles River Laboratories). Eggs allantoic fluid was snap frozen in ethanol-dry ice bath and stored at −80°C.

Experimental mice in studies were infected with MCMV by i.p. injection of 7.5×10^3 plaque-forming units (PFU) in 0.5 mL or by hydrodynamic injection (h.d.) of 4×10^4 PFU in 2.0 mL or by intranasal injection (i.n.) of 1×10^6 PFU in 0.05 mL. Hydrodynamic injection was performed as previously described[43] to deliver virus directly to the liver. In parabiotic experiments, both parabionts were infected with MCMV. In other studies, experimental mice were infected with SeV (Cantell Strain) by i.n. injection of 1×10^4 PFU or with Influenza (PR8-Strain) by i.n. injection of 5×10^2 PFU in 0.04 mL.

Virus quantification

MCMV viral titers were determined as previously described DNA[12]. was isolated from peripheral blood, PC, or Liver; using a genomic purification kit (QIAGEN). Following isolation, DNA concentration was measured using Nanodrop for each sample, and 3 μL was added into mastermix containing iQ Sybr Green (Bio-Rad) and primers specific to MCMV IE-1 DNA (F: TCGCCCATCGTTTCGAGA, R: TCTCGTAGGTCCACTGACGGA). Copy number was determined by comparing Cq values to a standard curve of known dilutions of an MCMV plasmid and normalized relative to total DNA content. Liver viral titers were normalized to weight of organ respectively.

Isolation of lymphocytes

Spleens were dissociated using glass slides and filtered through a 100-μm strainer. To isolate lymphocytes from liver, the tissues were physically dissociated using a glass tissue homogenizer and purified using a discontinuous gradient of 40% over 60% Percoll. To isolate cells from the lung, tissue was physically dissociated using scissors and incubated for 30 minutes in digest solution (1mg/ml type D collagenase in RPMI supplemented with 5% fetal calf serum, 1% L-glutamine, 1% penicillin-streptomycin, and 10 mM HEPES). Resulting dissociated tissue was passed through 100-μm strainers, centrifuged, and lymphocytes were removed from the supernatant. Red blood cells in spleen, lung, and liver were lysed using ACK lysis buffer.

Flow cytometry and cell sorting

Cell surface staining of single-cell suspensions from various organs was performed using fluorophore-conjugated antibodies (BD Biosciences, eBioscience, BioLegend, Tonbo, R&D Systems) as mentioned previously. Flow cytometry antibodies used in analysis of purified lymphocytes can be found below. Intracellular staining was performed by fixing and permeabilizing with the eBioscience Foxp3/Transcription Factor Staining Set for staining intranuclear proteins. *Ex vivo* Intracellular staining for IFN-γ was performed using the Cytofix/Cytoperm kit (BD Biosciences) after 5 hours incubation at 37°C of single cell suspension of lymphocytes in RPMI containing 10% fetal bovine serum with Brefeldin A (10 μg/mL, Sigma).

Flow cytometry and cell sorting were performed on the LSR II or Attune NxT, and Aria II cytometers (BD Biosciences), respectively. Data were analyzed with FlowJo software (Tree Star). Cell surface staining was performed using the following fluorophore-conjugated antibodies - NK1.1 (PK136), CD19 (ID3), CD49b/DX5 (DX5), KLRG1 (2F1), NKp46 (29A1.4), CD45.1 (A20), CD45 (30-F11), CD45.2 (104), CD8α (53–6.7), CD4 (GK1.5), TCRβ (H57–597), CD3e (17A2), Ly49H (3D10), CD200r1 (OX-110), CD49a (Ha31/8), IFN-γ (XMG1.2), F4/80 (BM8.1), CD11c (N418), CD11b (M1/70), Ly49D (4E5), Eomes (Dan11mag), IL-7rα (A7R34), IL-18rα (P3TUNYA), IL-2rα (PC61), Ki67 (Ki67).

ILC1s proliferation was analyzed by labeling sorted liver ILC1s with 5 mM CTV (Thermo Fisher) prior to transfer, and CTV labeling was performed according to manufacturer protocol. Apoptosis was evaluated by caspase activity staining using the carboxy-fluorescein

FLICA Poly Caspase Assay kit (ImmunoChemistry Technologies) according to manufacturer protocol.

Adoptive transfer experiments

ILC1s were purified from liver of CD45.2 wild-type mice by flow cytometric cell sorting to high purity and transferred into CD45.1 wild-type or CD45.1 Ly49H-deficient recipients and were infected with MCMV 1 day after adoptive transfer. In other experiments, naïve IL-18R^{-} ILC1 were purified from liver of CD45.2 wild-type mice by flow cytometric cell sorting to high purity and transferred into CD45.1 wild-type recipients and infected with MCMV 1 day following adoptive transfer. In other experiments, MCMV-experienced ILC1 were purified from the liver of CD45.2 wild-type mice by FACS cell sorting to high purity and transferred into naïve CD45.1 wild-type recipients.

Ex vivo stimulation of lymphocytes

Approximately 3×10^5 liver lymphocytes were stimulated for 5 hr in RPMI containing 10% fetal bovine serum with either recombinant mouse IL-12 (20 ng/ml; R&D Systems) plus IL-18 (10 ng/ml; R&D Systems), platebound αNK1.1 (PK136) or plate bound αNKp46 (29A1.4). Cells were cultured in media alone as a negative control.

RNA and ATAC Sequencing

For RNA sequencing, RNA was isolated from sorted cell populations from WT mice using TRIzol (Invitrogen) followed by SMARTer amplification and Illumina next-generation sequencing. For ATAC sequencing, ATAC-seq libraries were prepared as previously described[12]. FACS-sorted cell populations (1×10^4 cells) were lysed and accessible chromatin was transposed using Nextera Tn5 transposase. Transposed DNA fragments were isolated using Qiagen MinElute kit and amplified 5–10 cycles using Nextera PCR primers. ATAC-seq libraries were submitted for paired-end sequencing on Illumina Hiseq.

RNA and ATAC Sequencing Analysis

RNA and ATAC sequencing reads were aligned and pre-processed as described previously.[12] RNA sequencing reads were aligned using STAR (2.5.3a-foss-2016b) with filters --outFilterMultimapNmax 1 --outFilterMismatchNmax 999 --outFilterMismatchNoverLmax 0.02 --alignIntronMin 20 --alignIntronMax 1000000 --alignMatesGapMax 1000000 to allow for stringent alignment of unique reads to the mouse (mm10) genome[44]. Counts were made using BEDtools 2.27.1 coveragebed function. Raw count files were processed using DESeq2, removing genes with less than 50 counts. For ATAC sequencing peak-calling, read start sides aligned to the positive strand and negative strands were offset by +4bp and −5bp, respectively, as described by[45] Peak calling was performed on each time point (D0, D35 IL18^{+}) individually by pooling reads from biological replicates, and using MACS2[46], R137 with p-value threshold 0.2. To exclude any peaks identified due to noise, we calculated an irreproducible discovery rate (IDR)[47]. The IDR is an estimate of the threshold where two ranked lists of results, in this case peak calls ranked by P value, no longer represent reproducible events. Using this measure we excluded peaks that were not reproducible (IDR < 0.05) across replicates for each time point. We created a single atlas of accessible sites

across the two timepoints by merging peaks from the IDR-reproducible peak list for each timepoint. In this way, we created an atlas of 23016 reproducible peaks, and associated each peak to its nearest gene in the mouse genome. Differential expression and accessibility were computed using DESeq2; genes were considered differentially expressed at FDR p = 0.05 and absolute value of log2FC < 1, and peaks were considered differentially accessible between timepoints at FDR p = 0.2. For heatmaps, the R package pheatmap and Broad institute tool Morpheus was used to plot DESeq2 normalized counts. For visualization of tracks with IGV (IGV 2.3.94), BAM files were indexed with SAMtools/1.5-foss-2016b and then normalized by sequencing depth and converted to a BigWig file using Python/2.7.13-foss-2016b bamCoverage function. For GSEA analysis, T cell memory raw fastq files, from previously published data set of LCMV experienced T cell populations sort purified form the liver[32], were processed same as the ILC1 dataset. A list of differentially expressed genes was created compared to its corresponding naïve control. From this list, genes unique to each subset was used to create a gene list for GSEA analysis. The rank list input was created using the differentially expressed gene list and ordering them according to log(FC) values. A core memory signature was obtained by looking at differentially expressed genes upregulated between naïve and D35 IL-18R$^+$ ILC1 and identifying shared upregulated differentially expressed genes between naïve and memory T cell subsets from previously published data sets[32].

Statistical analyses

For graphs, data are shown as mean ± SEM, and unless otherwise indicated, statistical differences were evaluated using a Student's t test with Welch's correction to a assume a non-normal variance in our data distribution. $p < 0.05$ was considered significant. Graphs were produced and statistical analyses were performed using GraphPad Prism.

Reporting Summary

Further information on research design is available in the Nature Research Reporting Summary linked to this article.

Data Availability

The RNA-seq and ATAC-seq data is deposited in gene expression omnibus database under the accession number GSE128906. The data that support the findings of this study are available from the corresponding author upon request.

Supplementary Material

Refer to Web version on PubMed Central for supplementary material.

Acknowledgements

We thank members of the O'Sullivan, Leslie, Carlyle, Iwasaki and Sun labs for helpful comments and discussions. We thank J. Reichel and S. Jonjic for reagents. E.S. was supported by the NIH MSTP training grant (T32GM007205). N.M.A. was supported by a Medical Scientist Training Program Grant from the NIGMS of the NIH (T32GM007739 to the Weill Cornell/Rockefeller/Sloan Kettering Tri-Institutional MD-PhD Program) and an F30 Predoctoral Fellowship from NIAID of the NIH (F30 AI136239). J.C.S. was supported by the Ludwig Center

for Cancer Immunotherapy, the Burroughs Wellcome Fund, the American Cancer Society, and grants from the NIH (AI100874, AI130043, and P30CA008748). T.E.O. was supported by the NIH (P30DK063491, AI145997).

References

1. Henning AN, Roychoudhuri R & Restifo NP Epigenetic control of CD8(+) T cell differentiation. Nat Rev Immunol 18, 340–356 (2018). [PubMed: 29379213]
2. Youngblood B, Hale JS & Ahmed R T-cell memory differentiation: insights from transcriptional signatures and epigenetics. Immunology 139, 277–284 (2013). [PubMed: 23347146]
3. Bantug GR, Galluzzi L, Kroemer G & Hess C The spectrum of T cell metabolism in health and disease. Nat Rev Immunol 18, 19–34 (2018). [PubMed: 28944771]
4. Chang JT, Wherry EJ & Goldrath AW Molecular regulation of effector and memory T cell differentiation. Nat Immunol 15, 1104–1115 (2014). [PubMed: 25396352]
5. Schenkel JM & Masopust D Tissue-resident memory T cells. Immunity 41, 886–897 (2014). [PubMed: 25526304]
6. O'Sullivan TE, Sun JC & Lanier LL Natural Killer Cell Memory. Immunity 43, 634–645 (2015). [PubMed: 26488815]
7. Netea MG et al. Trained immunity: A program of innate immune memory in health and disease. Science 352, aaf1098 (2016). [PubMed: 27102489]
8. Martinez-Gonzalez I et al. Allergen-Experienced Group 2 Innate Lymphoid Cells Acquire Memory-like Properties and Enhance Allergic Lung Inflammation. Immunity 45, 198–208 (2016). [PubMed: 27421705]
9. Artis D & Spits H The biology of innate lymphoid cells. Nature 517, 293–301 (2015). [PubMed: 25592534]
10. Serafini N, Vosshenrich CA & Di Santo JP Transcriptional regulation of innate lymphoid cell fate. Nature reviews. Immunology 15, 415–428 (2015).
11. Kotas ME & Locksley RM Why Innate Lymphoid Cells? Immunity 48, 1081–1090 (2018). [PubMed: 29924974]
12. Weizman OE et al. ILC1 Confer Early Host Protection at Initial Sites of Viral Infection. Cell 171, 795–808 e712 (2017). [PubMed: 29056343]
13. Klose CSN et al. Differentiation of type 1 ILCs from a common progenitor to all helper-like innate lymphoid cell lineages. Cell 157, 340–356 (2014). [PubMed: 24725403]
14. Abt MC et al. Innate Immune Defenses Mediated by Two ILC Subsets Are Critical for Protection against Acute Clostridium difficile Infection. Cell Host Microbe 18, 27–37 (2015). [PubMed: 26159718]
15. Boulenouar S et al. Adipose Type One Innate Lymphoid Cells Regulate Macrophage Homeostasis through Targeted Cytotoxicity. Immunity 46, 273–286 (2017). [PubMed: 28228283]
16. Gasteiger G, Fan X, Dikiy S, Lee SY & Rudensky AY Tissue residency of innate lymphoid cells in lymphoid and nonlymphoid organs. Science 350, 981–985 (2015). [PubMed: 26472762]
17. Moro K et al. Interferon and IL-27 antagonize the function of group 2 innate lymphoid cells and type 2 innate immune responses. Nat Immunol 17, 76–86 (2016). [PubMed: 26595888]
18. Sun JC, Beilke JN & Lanier LL Adaptive immune features of natural killer cells. Nature 457, 557–561 (2009). [PubMed: 19136945]
19. Sun JC et al. Proinflammatory cytokine signaling required for the generation of natural killer cell memory. J Exp Med 209, 947–954 (2012). [PubMed: 22493516]
20. Beaulieu AM, Zawislak CL, Nakayama T & Sun JC The transcription factor Zbtb32 controls the proliferative burst of virus-specific natural killer cells responding to infection. Nat Immunol 15, 546–553 (2014). [PubMed: 24747678]
21. Zhou J et al. Liver-Resident NK Cells Control Antiviral Activity of Hepatic T Cells via the PD-1-PD-L1 Axis. Immunity (2019).
22. Best JA et al. Transcriptional insights into the CD8(+) T cell response to infection and memory T cell formation. Nat Immunol 14, 404–412 (2013). [PubMed: 23396170]

23. van der Veeken J et al. Memory of Inflammation in Regulatory T Cells. Cell 166, 977–990 (2016). [PubMed: 27499023]
24. Bradley LM, Haynes L & Swain SL IL-7: maintaining T-cell memory and achieving homeostasis. Trends Immunol 26, 172–176 (2005). [PubMed: 15745860]
25. Raeber ME, Zurbuchen Y, Impellizzieri D & Boyman O The role of cytokines in T-cell memory in health and disease. Immunol Rev 283, 176–193 (2018). [PubMed: 29664568]
26. Freeman BE, Hammarlund E, Raue HP & Slifka MK Regulation of innate CD8+ T-cell activation mediated by cytokines. Proc Natl Acad Sci U S A 109, 9971–9976 (2012). [PubMed: 22665806]
27. Kambayashi T, Assarsson E, Lukacher AE, Ljunggren HG & Jensen PE Memory CD8+ T cells provide an early source of IFN-gamma. J Immunol 170, 2399–2408 (2003). [PubMed: 12594263]
28. Bezman NA et al. Molecular definition of the identity and activation of natural killer cells. Nat Immunol 13, 1000–1009 (2012). [PubMed: 22902830]
29. Scott-Browne JP et al. Dynamic Changes in Chromatin Accessibility Occur in CD8(+) T Cells Responding to Viral Infection. Immunity 45, 1327–1340 (2016). [PubMed: 27939672]
30. Lau CM et al. Epigenetic control of innate and adaptive immune memory. Nat Immunol (2018).
31. Scharer CD, Bally AP, Gandham B & Boss JM Cutting Edge: Chromatin Accessibility Programs CD8 T Cell Memory. J Immunol 198, 2238–2243 (2017). [PubMed: 28179496]
32. Mackay LK et al. Hobit and Blimp1 instruct a universal transcriptional program of tissue residency in lymphocytes. Science 352, 459–463 (2016). [PubMed: 27102484]
33. Aguilar OA et al. A Viral Immunoevasin Controls Innate Immunity by Targeting the Prototypical Natural Killer Cell Receptor Family. Cell 169, 58–71 e14 (2017). [PubMed: 28340350]
34. Sun JC & Lanier LL The Natural Selection of Herpesviruses and Virus-Specific NK Cell Receptors. Viruses 1, 362 (2009). [PubMed: 20151027]
35. Snyder CM et al. Memory inflation during chronic viral infection is maintained by continuous production of short-lived, functional T cells. Immunity 29, 650–659 (2008). [PubMed: 18957267]
36. Arase H, Mocarski ES, Campbell AE, Hill AB & Lanier LL Direct recognition of cytomegalovirus by activating and inhibitory NK cell receptors. Science 296, 1323–1326 (2002). [PubMed: 11950999]
37. O'Leary JG, Goodarzi M, Drayton DL & von Andrian UH T cell- and B cell-independent adaptive immunity mediated by natural killer cells. Nat Immunol 7, 507–516 (2006). [PubMed: 16617337]
38. Paust S et al. Critical role for the chemokine receptor CXCR6 in NK cell-mediated antigen-specific memory of haptens and viruses. Nat Immunol 11, 1127–1135 (2010). [PubMed: 20972432]
39. Peng H et al. Liver-resident NK cells confer adaptive immunity in skin-contact inflammation. J Clin Invest 123, 1444–1456 (2013). [PubMed: 23524967]
40. Cooper MA et al. Cytokine-induced memory-like natural killer cells. Proc Natl Acad Sci U S A 106, 1915–1919 (2009). [PubMed: 19181844]
41. Quintin J et al. Candida albicans infection affords protection against reinfection via functional reprogramming of monocytes. Cell Host Microbe 12, 223–232 (2012). [PubMed: 22901542]
42. Min-Oo G & Lanier LL Cytomegalovirus generates long-lived antigen-specific NK cells with diminished bystander activation to heterologous infection. J Exp Med 211, 2669–2680 (2014). [PubMed: 25422494]

Methods-only References

43. Liu F, Song Y & Liu D Hydrodynamics-based transfection in animals by systemic administration of plasmid DNA. Gene therapy 6, 1258–1266 (1999). [PubMed: 10455434]
44. Tokuyama M et al. ERVmap analysis reveals genome-wide transcription of human endogenous retroviruses. Proc Natl Acad Sci U S A 115, 12565–12572 (2018). [PubMed: 30455304]
45. Buenrostro JD, Giresi PG, Zaba LC, Chang HY & Greenleaf WJ Transposition of native chromatin for fast and sensitive epigenomic profiling of open chromatin, DNA-binding proteins and nucleosome position. Nat Methods 10, 1213–1218 (2013). [PubMed: 24097267]
46. Zhang Y et al. Model-based analysis of ChIP-Seq (MACS). Genome Biol 9, R137 (2008). [PubMed: 18798982]

47. Zigler CM & Belin TR The Potential for Bias in Principal Causal Effect Estimation When Treatment Received Depends on a Key Covariate. Ann Appl Stat 5, 1876–1892 (2011). [PubMed: 22308190]

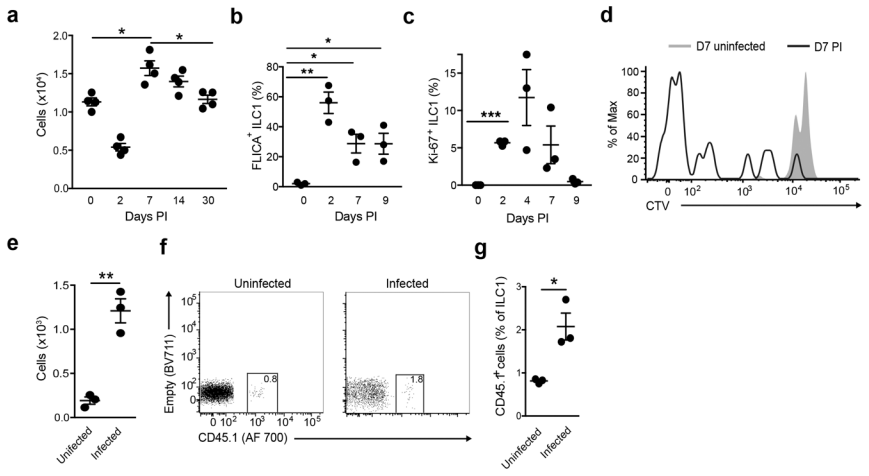

Figure 1. Liver-resident ILC1s robustly proliferate and persist following MCMV infection.

(a) Absolute cell numbers of Lin$^-$NK1.1$^+$CD49b$^-$Eomes$^-$CD200r1$^+$ ILC1s (hereafter ILC1s) in the liver of 8 week old C57BL/6 wild-type (WT) mice infected with MCMV intraperitoneally (i.p.) at the indicated time points post-infection as determined by flow cytometry. Lin=CD3ε$^+$TCRβ$^+$CD19$^+$F4/80$^+$. **(b,c)** The incorporation of FLICA **(b)** and the quantification of Ki67 staining by percentage **(c)** in ILC1s in the liver of at indicated time points following MCMV infection i.p. **(d,e)** Representative histogram of cell trace violet (CTV) dilution **(d)** and quantification of cell numbers **(e)** of adoptively transferred CD45.2$^+$ ILC1s into CD45.1 WT hosts recovered in the liver 7 days after MCMV infection (i.p), compared to uninfected controls. **(f-g)** Representative plots **(f)** and percentage **(g)** of 4×10^4 adoptively transferred CD45.2$^+$ ILC1s recovered in the liver of CD45.1 WT mice injected with MCMV (i.p) or PBS at 30 days post-injection. Data are representative of 3 independent experiments with **(a)** n=4 mice and **(b-g)** n=3 mice per group. Samples were compared a two-tailed Student's t test, and data are presented as the mean ± SEM (*p<0.05, **p<0.01).

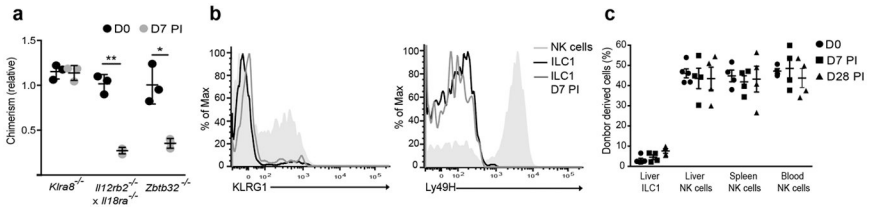

Figure 2. Liver ILC1s locally proliferate in a proinflammatory cytokine-dependent manner following MCMV infection.

(a) Relative chimerism shown as ratio of indicated surface receptor or transcription factor deficient ILC1s (CD45.2$^+$) to WT ILC1s (CD45.1$^+$) in the liver of reconstituted mixed bone marrow chimeras at indicated time points following MCMV infection (i.p). **(b)** Histograms of indicated cell surface markers of uninfected WT Lin$^-$NK1.1$^+$Eomes$^+$CD49b$^+$CD200r$^-$ NK cells (hereafter NK cells), uninfected WT ILC1s, and 4×10^4 adoptively transferred CD45.2$^+$ liver ILC1s recovered in the liver of CD45.1 Ly49H-deficicent host infected with MCMV (i.p) at 7 days post-infection. **(c)** Percentage of donor derived NK cells and ILC1s shown for indicated organs of parabiotic mice were infected with MCMV (i.p), at indicated time points following infection. Data are representative of 3 independent experiments with **(a,b)** n=3 mice and **(c)** n=4 parabiotic pairs per group. Samples were compared using two-tailed Student's t test, and data are presented as the mean ± SEM (*p<0.05, **p<0.01).

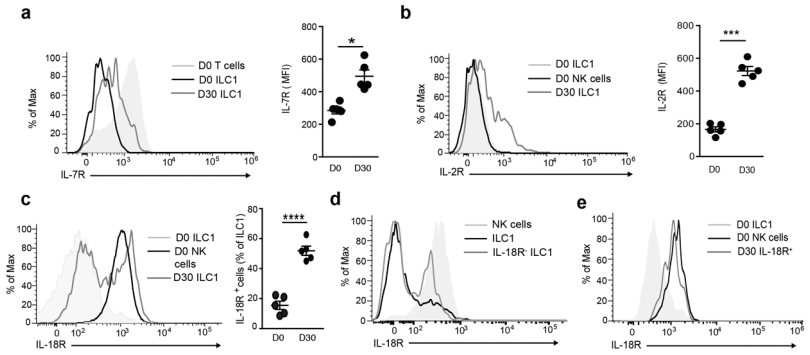

Figure 3. MCMV-experienced liver ILC1s increase the expression of cytokine receptors *in vivo*.

(a) Representative histogram of T Cells (TCRβ^{+}CD3ε $^{+}$NK1.1^{-}) and ILC1s and quantification of ILC1s for IL-7R MFI in the liver of WT mice uninfected or infected with MCMV intraperitoneally (i.p.) at the indicated time points post-infection. **(b,c)** Representative histogram of NK cells and ILC1s and quantification of ILC1s for IL-2R MFI **(b)** and frequency of IL-18R^{+} ILC1s **(c)** in the liver of wild-type (WT) mice uninfected or infected with MCMV intraperitoneally (i.p.) at the indicated time points post-infection. **(d)** Representative histogram of 4×10^{4} adoptively transferred CD45.2^{+} IL-18R^{-} ILC1s recovered in the liver of CD45.1 WT recipient mice infected with MCMV (i.p) at 7 days post-injection. **(e)** Representative histogram of IL-18R staining on uninfected NK cells, uninfected ILC1s, and adoptively transferred sort purified 4×10^{4} CD45.2^{+} IL-18R^{+} ILC1s from the liver of day 35 MCMV infected WT mice recovered in CD45.1 WT recipients three days after transfer. Data are representative of 3 independent experiments with **(a-c)** n=5 mice and **(d,e)** n=4 mice per group. Samples were compared using two-tailed Student's t test, and data are presented as the mean ± SEM (*p<0.05,***p<0.001, ****p<0.0001).

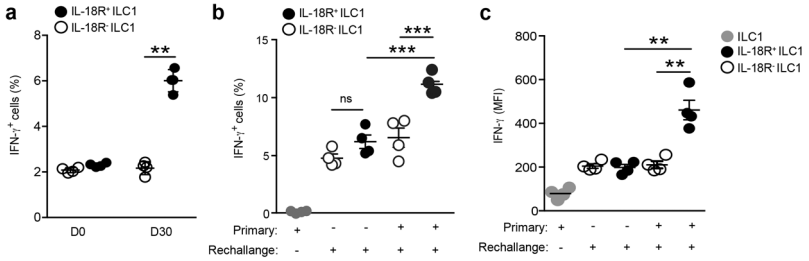

Figure 4. IL-18R^{+} ILC1s display enhanced IFN-γ production following secondary MCMV challenge.

(a) Graph shows percentage of IFN-γ^{+} cells within indicated liver ILC1s at indicated time points following MCMV i.p. infection in WT mice, following plate-bound stimulation with either media alone or αNK1.1 antibody. **(b,c)** Quantification of *ex vivo* intracellular IFN-γ staining by percentage **(b)** and MFI **(c)** of indicated liver ILC1s populations at 24 hours after MCMV challenge in *Rag2*$^{-/-}$ mice that were injected initially with PBS or MCMV i.p. and were subsequently challenged 28 days PI with MCMV hydrodynamically (h.d.). Data are representative of 3 independent experiments with **(a)** n=3 mice and **(b,c)** n=4 mice per group. Samples were compared using two-tailed Student's t test, and data are presented as the mean ± SEM (**p<0.01,***p<0.001).

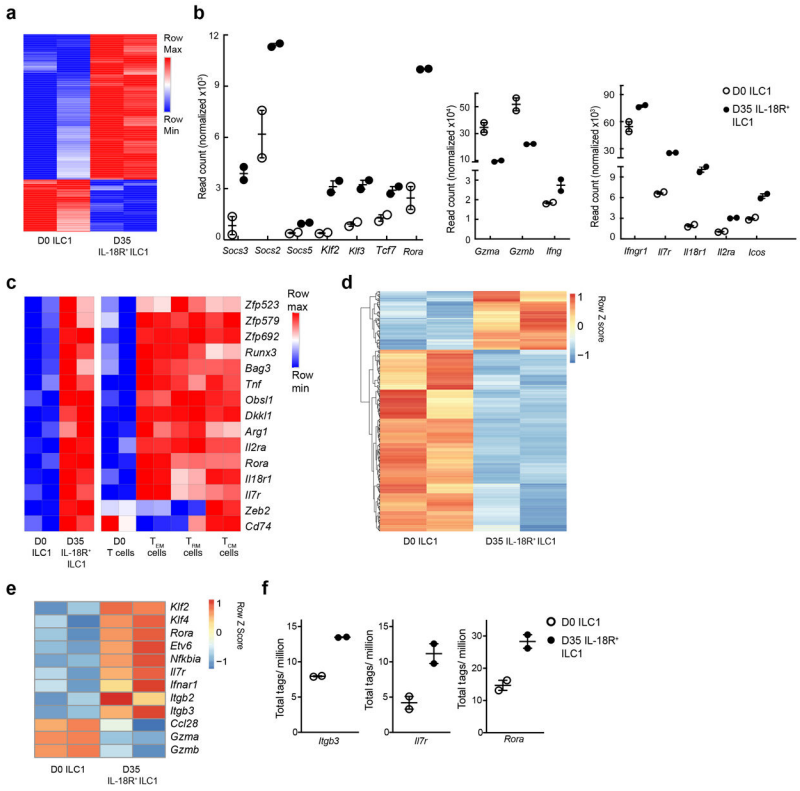

Figure 5. A distinct genome-wide transcriptional and chromatin landscape defines a distinct IL-18R^{+} ILC1 subset.

(a) Differential gene expression heat map across all samples for top 500 DE genes (FDR-adjusted p-value<0.05; absLog2FC > 1) in liver ILC1s sort purified from wild-type mice and analyzed by RNA-seq at the indicated time points following infection; **(b)** Normalized read count of samples indicated by a manually curated representative subset from dataset shown in (**a**). **(c)** Heat map of core memory signature shared between ILC1s and memory T cell subsets (see methods) assessed by RNA-sequencing as was previously reported [32]; **(d)** Chromatin accessibility heat map across all samples for all genes with FDR-adjusted p-value less than 0.2 (373 total) in liver ILC1s sort purified from wild-type mice and analyzed by ATAC-seq at the indicated time points following infection. **(e)** Differentially accessible peak signature of all samples indicated by a manually curated representative subset from dataset shown in (**d**). **(f)** Quantification of peaks mapping to promoter peaks (1.5 kb upstream and downstream of the transcriptional start site) for *Itgb3, Il7r,* and *Rora* for all samples. Data are representative of 2 replicate experiments with n=2 samples of n=20 pooled mice per condition. All adjusted p values were indeed determined using DESeq2 and were two-sided. Data are presented as as the mean ± SEM.

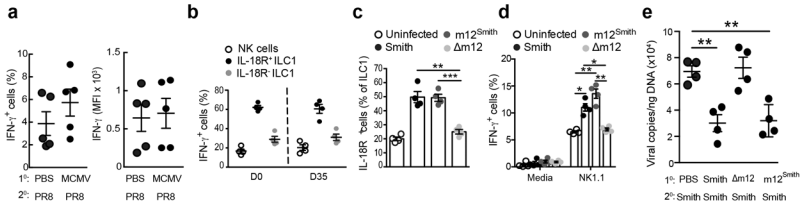

Figure 6. The MCMV-encoded protein m12 preferentially drives formation of IL-18R$^+$ ILC1s.

(a) Quantification of *ex-vivo* intracellular IFN-γ staining by percentage and MFI of ILC1s at 48 hours following Influenza-PR8 challenge in i.v. CD45 unlabeled fraction of the lung in WT mice that were injected initially with either PBS or MCMV intranasally (i.n.) and 28 days later subsequently challenged with Influenza-PR8 (i.n.). **(b)** Quantification of IFN-γ$^+$ cells within indicated liver ILC1 populations from WT mice infected with MCMV-Smith ip and analyzed 35 days PI compared to uninfected controls following stimulation with IL-12 and IL-18; **(c-d)** Quantification of percentage of IL-18R expressing liver ILC1**(c)** and quantification of intracellular IFN-γ staining in IL18R$^+$ ILC1 **(d)** in WT mice that were infected with indicated MCMV strains i.p and analyzed 30 days PI, following stimulation with either media alone or plate-bound αNK1.1 antibody. (**e**) Viral titers of 36 hours post-infection of liver tissue lysate of *Rag2*$^{-/-}$ mice primed with either m12 sufficient or deficient MCMV strains (i.p.) and challenged 28 days later with Smith strain by h.d. injection. Data are representative of 3 independent experiments with **(a)** n=5 mice and **(b-e)** n=4 mice per group. Samples were compared using two-tailed Student's t test, and data are presented as the mean ± SEM (*p<0.05, **p<0.01, ***p<0.001)